

Study of Excited Ξ Baryons in $\bar{p}p$ -Collisions with $\overline{\text{PANDA}}$

Authors:

Jennifer Pütz, Albrecht Gillitzer, James Ritman

Abstract

Understanding the excitation pattern of baryons is indispensable for a deep insight into the mechanism of non-perturbative QCD. Up to now only the nucleon excitation spectrum has been subject to systematic experimental studies while very little is known on excited states of double or triple strange baryons.

In studies of antiproton-proton collisions the $\overline{\text{PANDA}}$ experiment is well-suited for a comprehensive baryon spectroscopy program in the multi-strange and charm sector. A large fraction of the inelastic $\bar{p}p$ cross section is associated to final states with a baryon-antibaryon pair together with additional mesons, giving access to excited states both in the baryon and the antibaryon sector.

In the present study we focus on excited Ξ states. For final states containing a $\Xi \bar{\Xi}$ pair cross sections up to the order of μb are expected, corresponding to production rates of $\sim 10^6/\text{d}$ at a Luminosity $L = 10^{31} \text{ cm}^{-2} \text{ s}^{-1}$ (5% of the full value). A strategy to study the excitation spectrum of Ξ baryons in antiproton-proton collisions will be discussed. The reconstruction of reactions of the type $\bar{p}p \rightarrow \Xi^* \bar{\Xi}$ (and their charge conjugated) with the $\overline{\text{PANDA}}$ detector will be presented based on a specific exemplary reaction and decay channel.

Contents

1	Motivation	1
2	Event generation	2
3	Analysis	6
3.1	Final state particle	6
3.2	Reconstruction of Λ^0 and $\bar{\Lambda}^0$	6
3.2.1	Combination	6
3.2.2	Fitting	8
3.2.3	Results	8
3.3	Reconstruction of Ξ and $\bar{\Xi}$	12
3.3.1	Combination	12
3.3.2	Fitting	12
3.3.3	Results	12
3.4	Reconstruction of $\Xi(1820)$ and $\bar{\Xi}(1820)$	18
3.4.1	Combination	18
3.4.2	Fitting	18
3.5	Reconstruction of hole chain	18
3.5.1	combination	18
3.5.2	Fitting	18
4	Background	21
	Literature	22

1 Motivation

2 Event generation

first key words!!!!

- parameter for evt generation table 2.1

Table 2.1: Parameter for event generation

Parameter	Value
Beam momentum	4.6 GeV/c ²
Production	PHSP
Tracking	Ideal
Particle ID	Ideal

- beam momentum: 100 MeV over threshold
- assumed: highest cross section (Quelle!!!!!!)
- Software Framework: Pandaroot 2.2

Table 2.2: Used software versions

Software	Version
FairSoft	mar15
FairRoot	v-15.03a
PandaRoot	trunk revision 28555
Geant	3
Genfit	1

- for signal: 1.5 Mio events
- decay channel shown in picture 2.1
- add particle to evt.pdl (code sniplet 2.1 with values table 2.3 from [1] (Source!!!!))

Listing 2.1: sniplet from evt.pdl

Table 2.3: Values for $\Xi(1820)^-$ and $\bar{\Xi}(1820)$ from [1]

Particle	J	I	P	Charge	Mass	Width
$\Xi(1820)^-$	$\frac{3}{2}$	$\frac{1}{2}$	(-1)	(-1)	$(1.823 \pm 5)\text{GeV}/c^2$	$(0.024 \pm 6)\text{ GeV}$
$\bar{\Xi}(1820)$	$\frac{3}{2}$	$\frac{1}{2}$	(-1)	1	$(1.823 \pm 5)\text{GeV}/c^2$	$(0.024 \pm 6)\text{ GeV}$

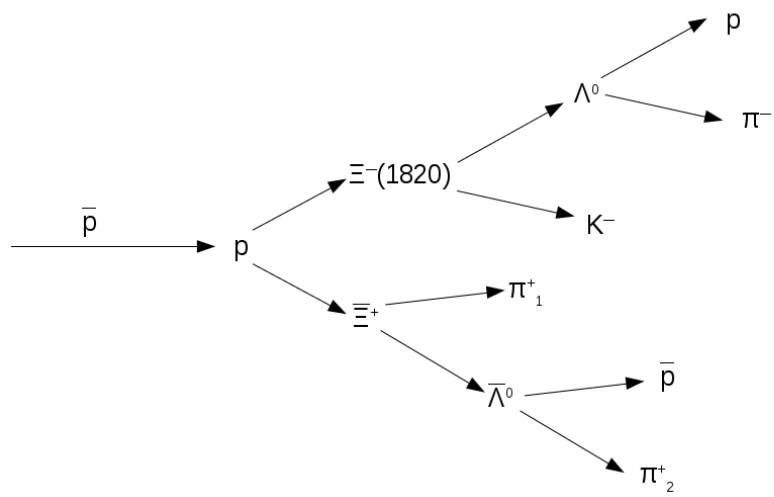


Figure 2.1: Simulated decay channel

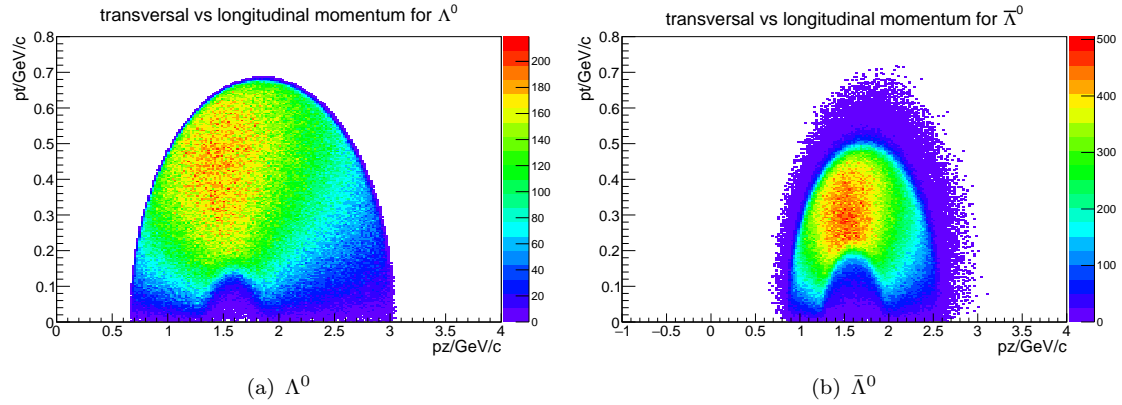


Figure 2.2: Figure a) shows transversal against the longitudinal momentum distribution for Λ^0 . Figure b) transversal versus longitudinal momentum distribution for $\bar{\Lambda}^0$.

```
add p Particle Xi(1820)- 23314 1.8230000e+00 2.4000000e-02
    2.0000000e-01 -3 3 0.0000000e+00 23314
add p Particle anti-Xi(1820)+ -23314 1.8230000e+00 2.4000000e-02
    2.0000000e-01 3 3 0.0000000e+00 -23314
```

- plot of transverse momentum against longitudinal momentum in figure 2.2
- Dalitz plots for simulation figure 2.4

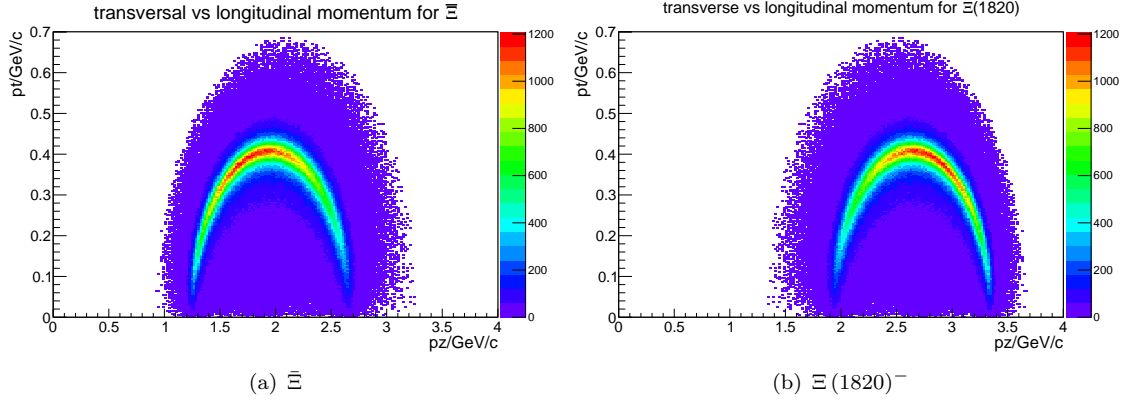


Figure 2.3: Figure a) shows transversal against the longitudinal momentum distribution for Ξ^- . Figure b) transversal versus longitudinal momentum distribution for $\Xi(1820)^-$.

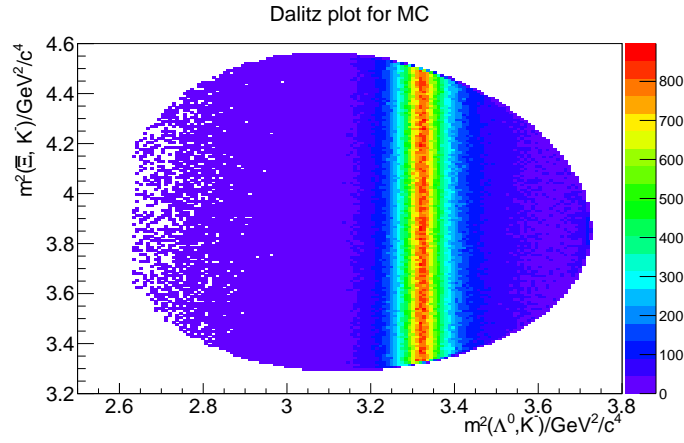


Figure 2.4: Dalitz plot for simulation. On x axis is the mass square of Λ^0 and K^- and on the y axis there is the mass square of Ξ^- and K^-

3 Analysis

Here is all the stuff of the analysis!

3.1 Final state particle

- final state particle: proton, antiproton, π^- , π^+ , K^- and K^+ mesons
 - reconstructed in Detector
 - only particles with more then 3 hits either in any of the tracking detectors MVD, STT or GEM
 - reason: 3 hits define circle; fourth hit point gives a validation for track hypothesis
 - ideal PID (reason!!!)
 - reco efficiency in table 3.1 see also figure 3.1
 - for c.c. channel see table 3.2

3.2 Reconstruction of Λ^0 and $\bar{\Lambda}^0$

3.2.1 Combination

- only final state particle with more than 3 Hits
 - daughter particles for Λ^0 : proton an π^- meson
 - daughter particles for $\bar{\Lambda}^0$: \bar{p} and π^+ here π_2^+
 - for c.c. chain: Λ^0 : proton and π_2^- ; $\bar{\Lambda}^0$: \bar{p} and π^+
 - performing a mass window cut with width of $0.3\text{GeV}/c^2$

Table 3.1: reco efficiency and momentum resolution for $\bar{p}p \rightarrow \Xi(1820)^- \bar{\Xi}$

final state	N/%	$\frac{\sigma_p}{p}/\%$
π^-	83.48	1.53
π_1^+ ($\bar{\Xi}$)	80.93	1.38
π_2^+ ($\bar{\Lambda}^0$)	83.07	1.49
K^-	78.59	1.58
p	84.39	1.61
\bar{p}	78.25	1.61

Table 3.2: reco efficiency and momentum resolution for $\bar{p}p \rightarrow \bar{\Xi}(1820) \Xi$

final state	N/%	$\frac{\sigma p}{p}/\%$
π^+		
$\pi_1^- (\Xi)$		
$\pi_2^- (\Lambda^0)$		
K^+		
p		
\bar{p}		

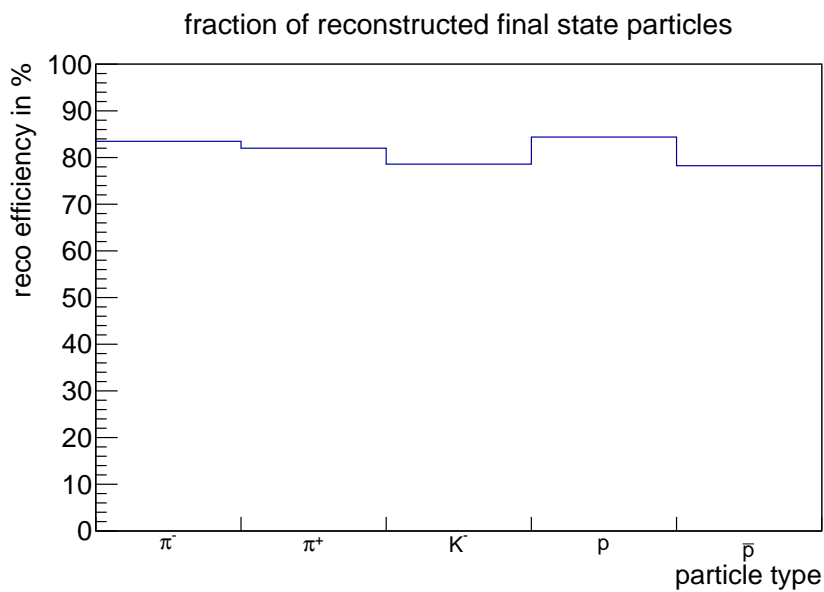


Figure 3.1: Reconstruction efficiency for final state particles. The x axis shows the particle type. On the y axis is shown the fraction of reconstructed particles, like it is shown in table 3.1

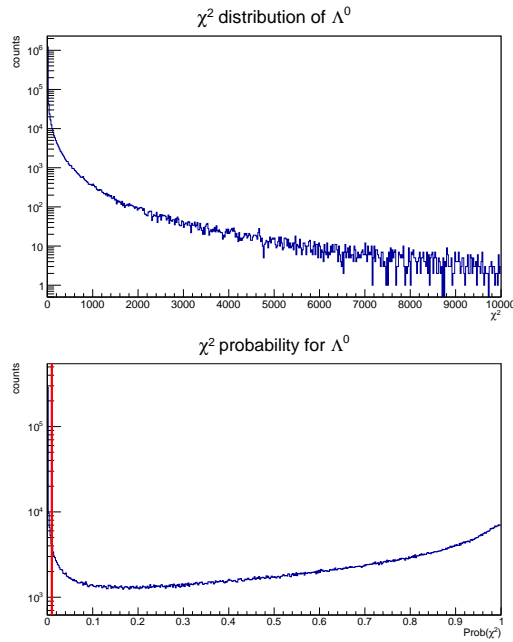


Figure 3.2: upper: χ^2 distribution; lower: χ^2 probability distribution

3.2.2 Fitting

- fitting particles to common vertex with PndKinVtxFitter
 - χ^2 and χ^2 -Probability distribution shown in figure 3.2
 - features in probability distribution are not coming from vertex fitting. There is still a problem with covariance matrices.
 - fit information are given to PndKinFitter with mass constraint
 - only select particles with prob bigger than 0.01 for both fitters
 - scheme in figure 3.3
 - if there is more than one particle, choose best candidate

3.2.3 Results

- mass distribution for different cuts see figure 3.4 and figure 3.5
 - performing a double gaussian fit on cutted mass for Λ^0 and $\bar{\Lambda}^0$ (example see figure 3.6)
 - result of massfit $m = (1.116 \pm 3.5 \cdot 10^{-5}) \text{ GeV}/c^2$
 - small error seems to come from wrong covariance matrices.
 - transverse vs longitudinal momentum shown in figure 3.7
 - the reconstruction efficiency for Λ^0 is 50.33% and for $\bar{\Lambda}^0$ 41.46%
 - reason: Λ^0 is emitted by $\Xi(1820)^-$ which has a very little decay length; lambda decay length is $c\tau = 7.98 \text{ cm}$ [1]; Λ^0 decays in MVD detector; high precision for reconstructed

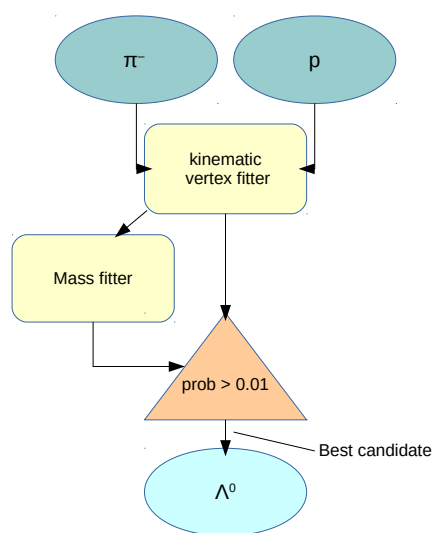


Figure 3.3: Scheme for Λ^0 reconstruction

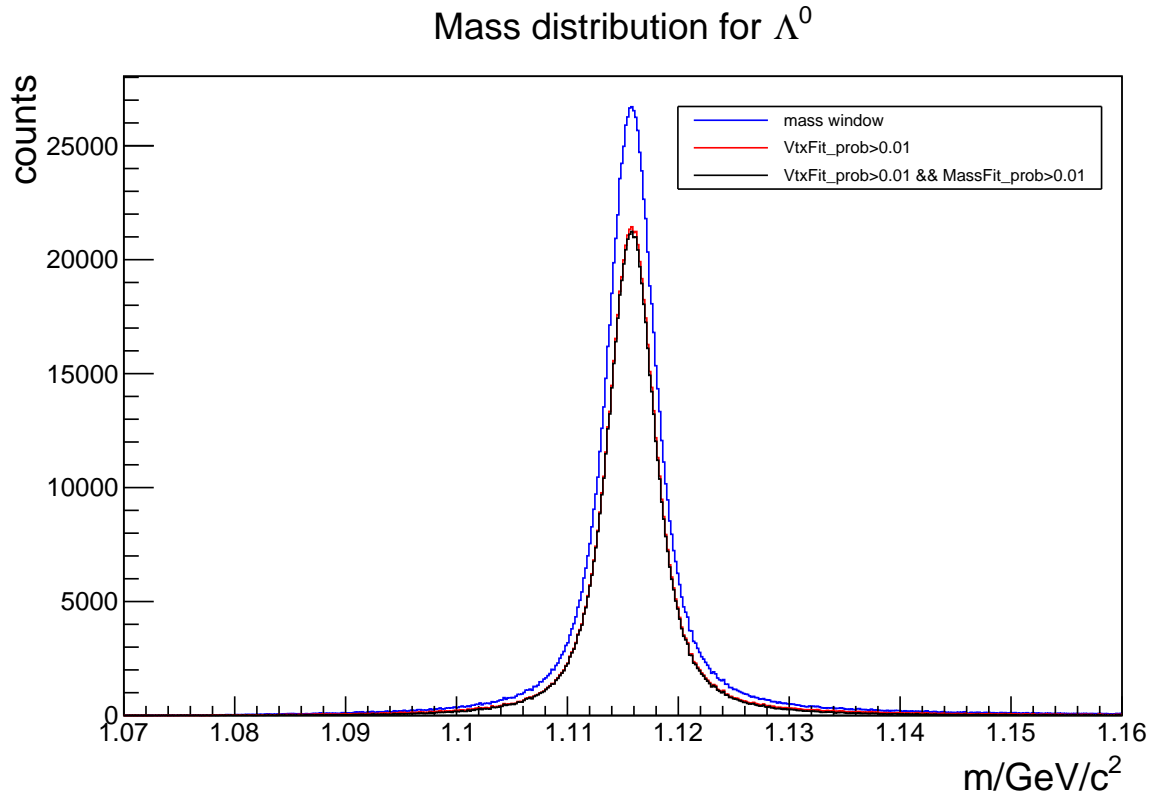


Figure 3.4: Mass distribution of Λ^0 for different cuts

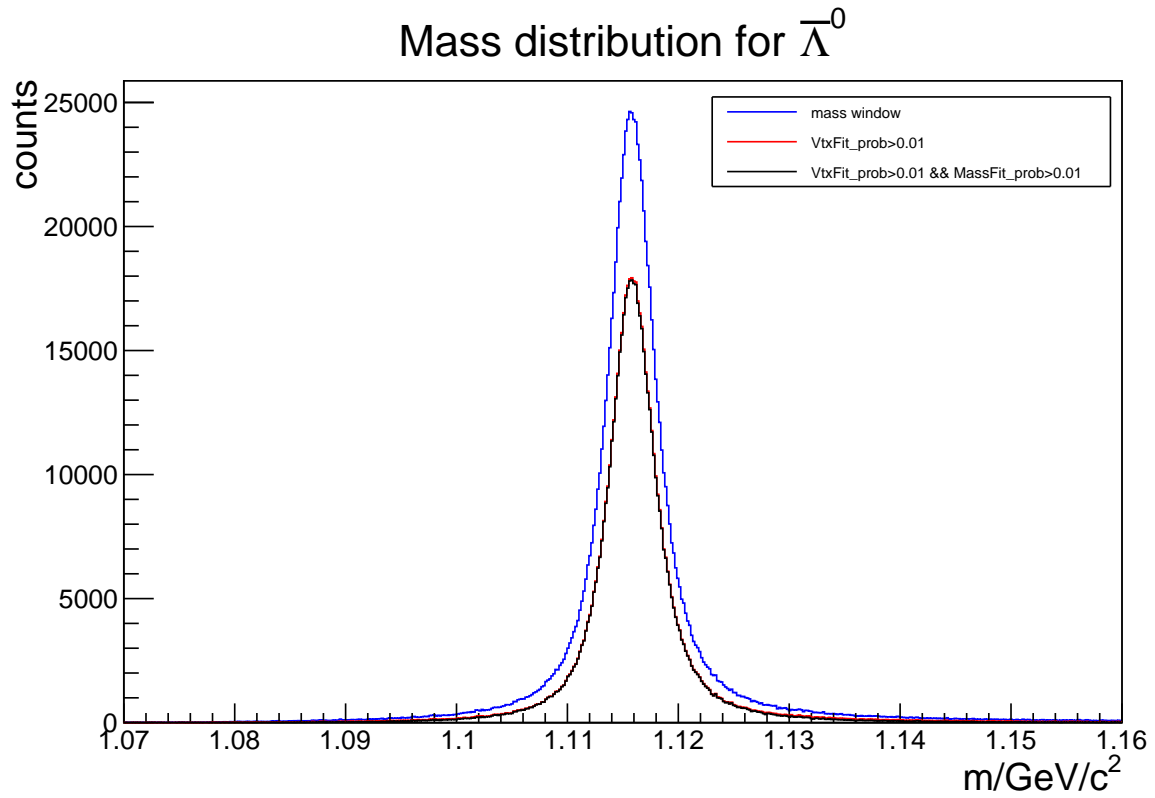


Figure 3.5: Mass distribution of $\bar{\Lambda}^0$ for different cuts

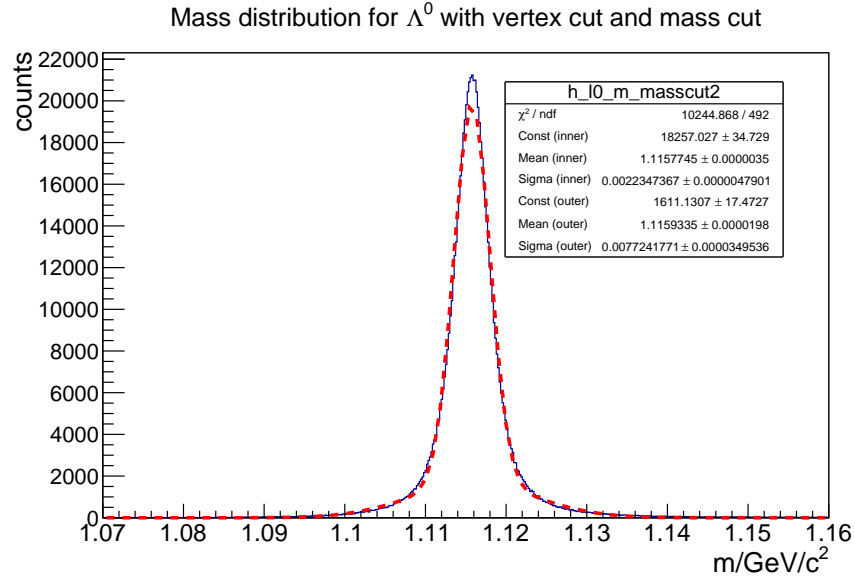


Figure 3.6: Mass fit with a double gaussian fit

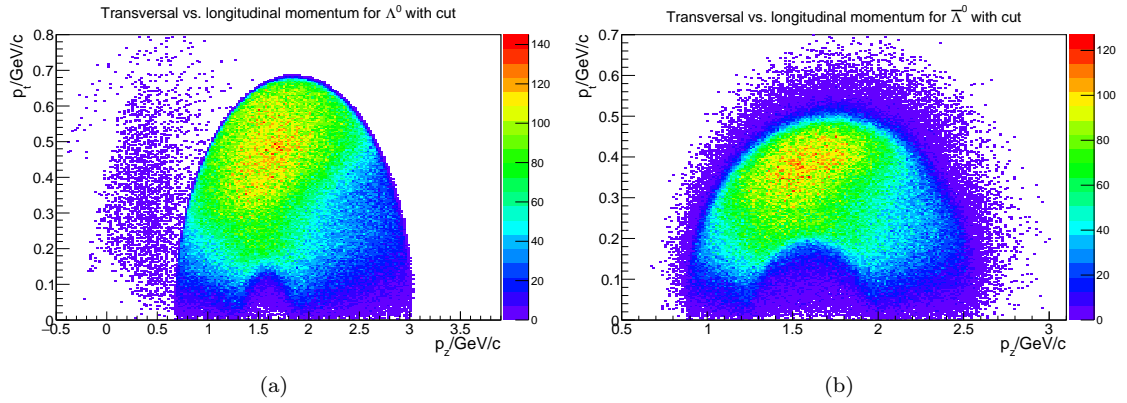


Figure 3.7: The plots shows the transverse against the longitudinal momentum for Λ^0

Table 3.3: Vertex resolution for Ξ^- and Ξ^0 (c.c. channel)

position	Ξ^-	cascade(from c.c.)
x	0.03282 ± 0.00017	
y	0.03326 ± 0.00017	
z	0.12054 ± 0.00058	

final state particles; $\bar{\Lambda}^0$ is produced by Ξ^- which has a decay length of $c\tau = 4.91$ cm; $\bar{\Lambda}^0$ is produced deep in MVD, so that final state particles coming from $\bar{\Lambda}^0$ are produced at the edge of the MVD detector. See figure 3.8

3.3 Reconstruction of Ξ^- and Ξ^0

3.3.1 Combination

- similar scheme for Λ^0 and $\bar{\Lambda}^0$
 - daughter particles for Ξ^- : $\bar{\Lambda}^0$ and π^+ here π_1^+
 - daughter particles for Ξ^0 : Λ^0 and π^- meson here π_1^-
 - using best candidate from Λ^0 and $\bar{\Lambda}^0$
 - performing a mass window cut with width of $0.3\text{GeV}/c^2$ means $m_{\Xi} \pm 0.15 \text{ GeV}/c^2$ with $m_{\Xi} = 1.32171 \text{ GeV}/c^2$ [1]

3.3.2 Fitting

- fitting particles to common vertex with PndKinVtxFitter
 - fit information are given to PndKinFitter with mass constraint
 - scheme in figure 3.9
 - only select particles with prob bigger than 0.01 for both fitters (figure 3.10)
 - if there is more than one particle, choose best candidate
 - vertex resolution shown in table 3.3
 - vertex resolution is determined by using a double Gaussian fit; "inner" σ is vertex resolution, see figure 3.11 and figure 3.12

3.3.3 Results

- mass distribution for different cuts see figure 3.13 and figure 3.14
 - performing a double gaussian fit on cutted mass for Ξ^- and Ξ^0 (example see figure 3.15)
 - result of massfit $m = (1.3721716 \pm 9.2 \cdot 10^{-5}) \text{ GeV}/c^2$
 - small error seems to come from wrong covariance matrices.
 - transverse vs longitudinal momentum for Ξ^- and Ξ^0 is shown in figure 3.16

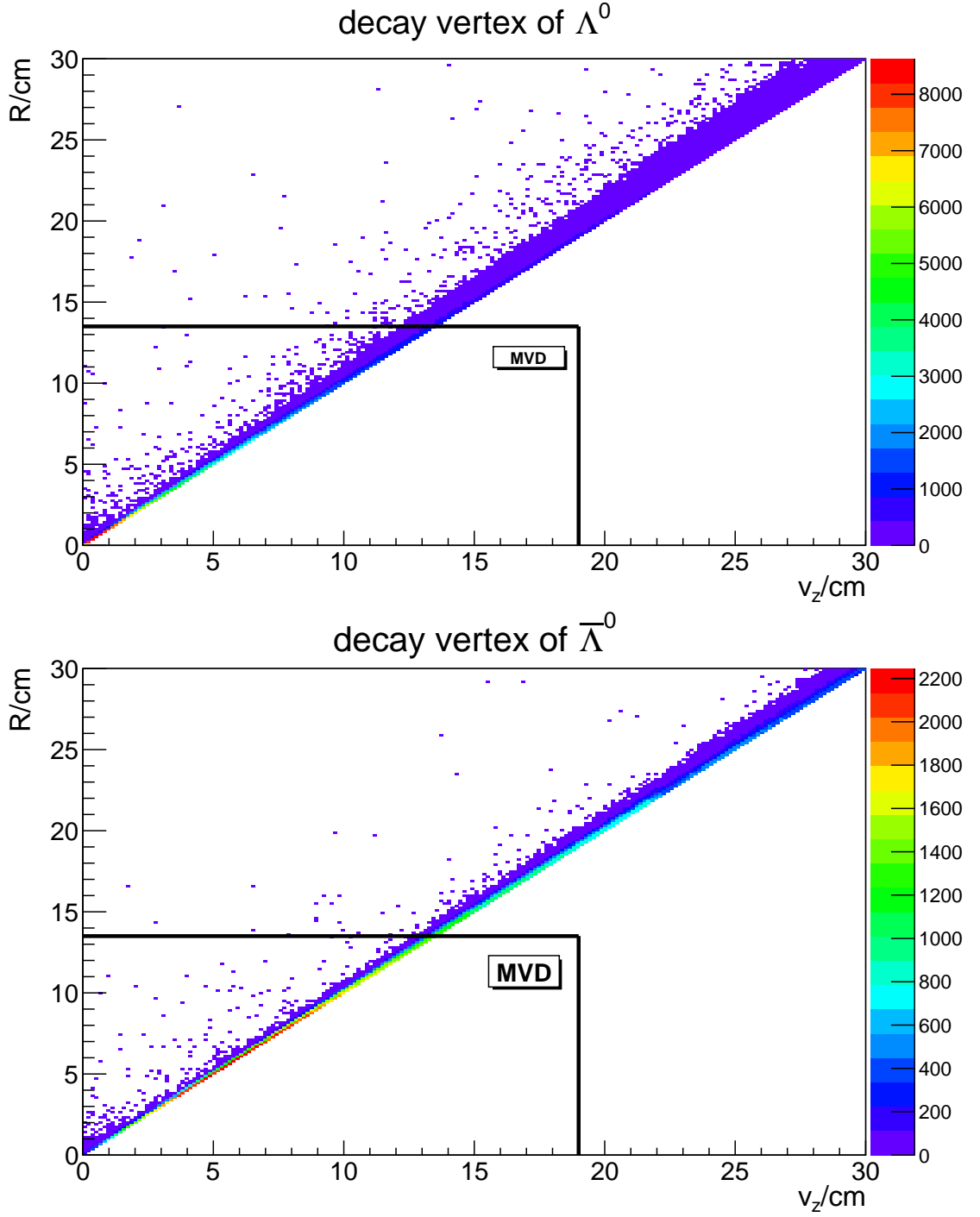


Figure 3.8: Upper plot shows the decay vertex of Λ^0 ; lower plot shows decay vertex of $\bar{\Lambda}^0$

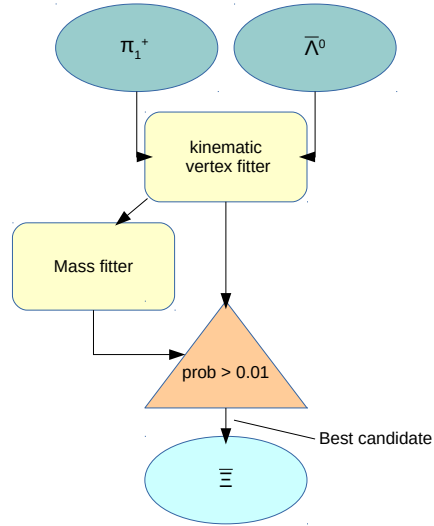


Figure 3.9: Scheme for Ξ reconstruction

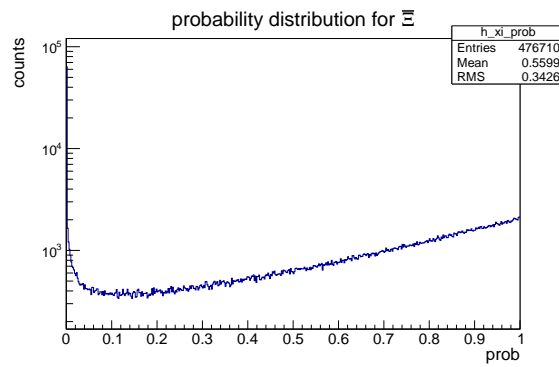


Figure 3.10: χ^2 probability for Ξ reconstruction

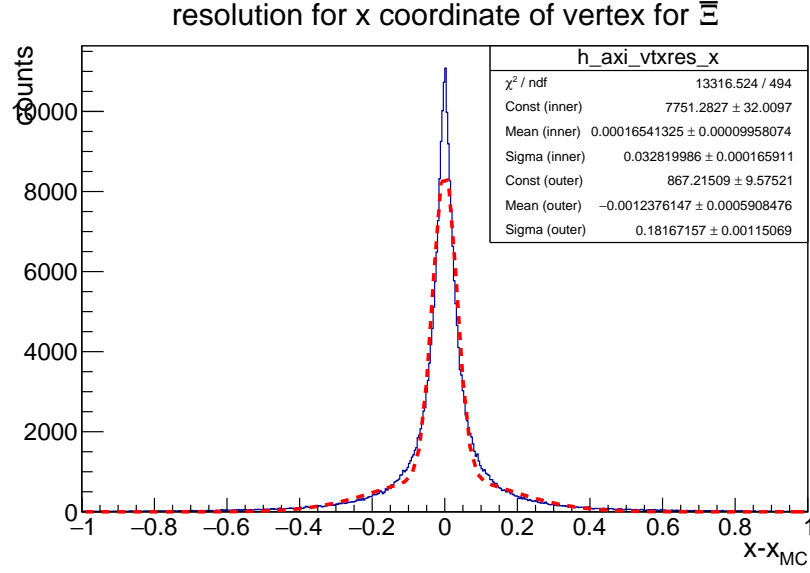


Figure 3.11: Vertex resolution of x position for Ξ

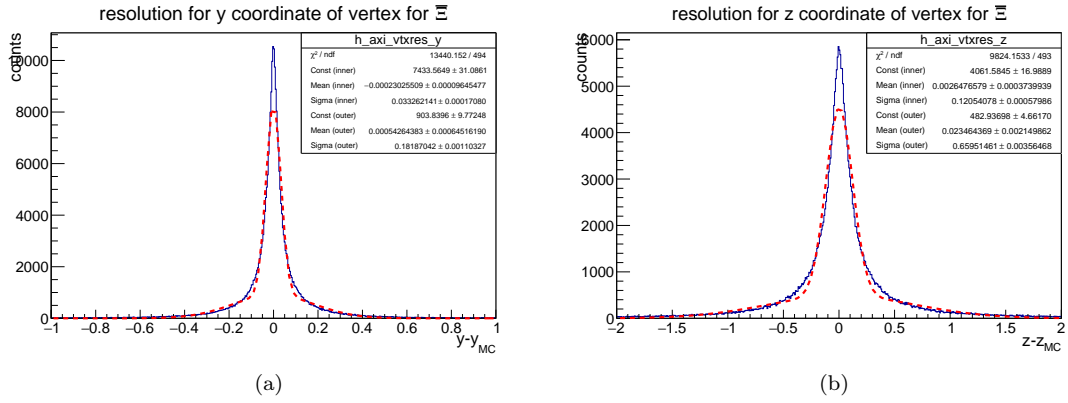


Figure 3.12: left plot: Vertex resolution of y position for Ξ ; right plot: Vertex resolution of z position for Ξ .

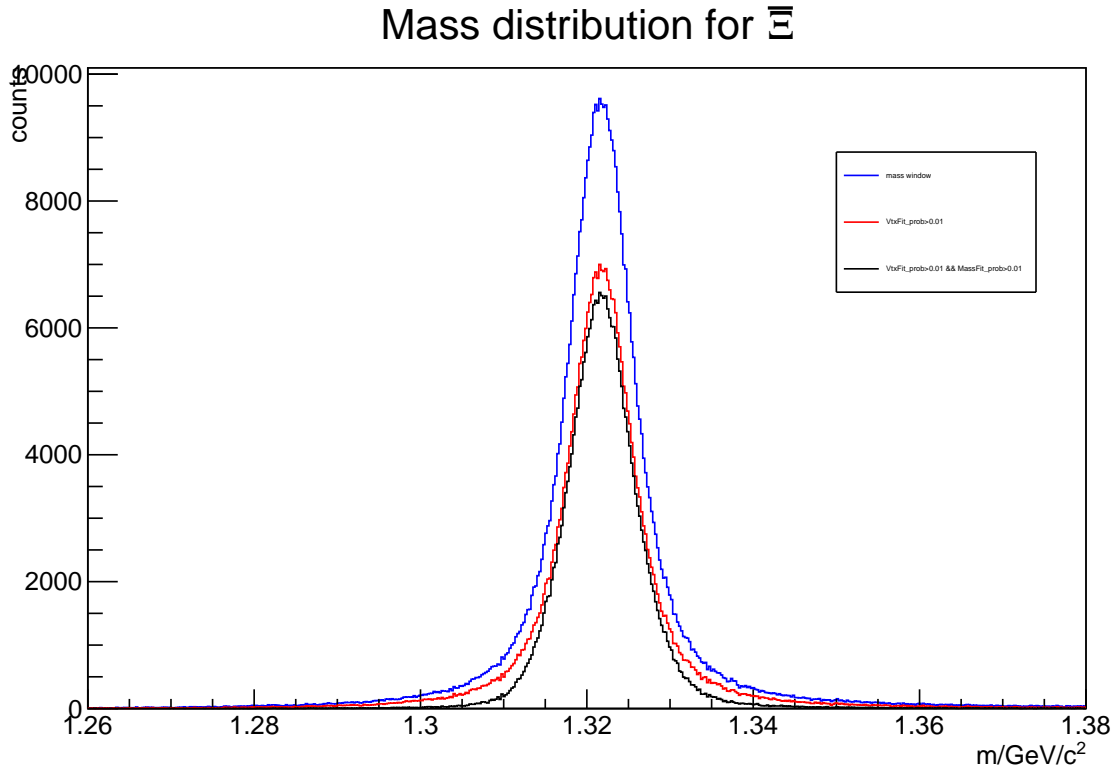


Figure 3.13: Mass distribution of Ξ^- for different cuts

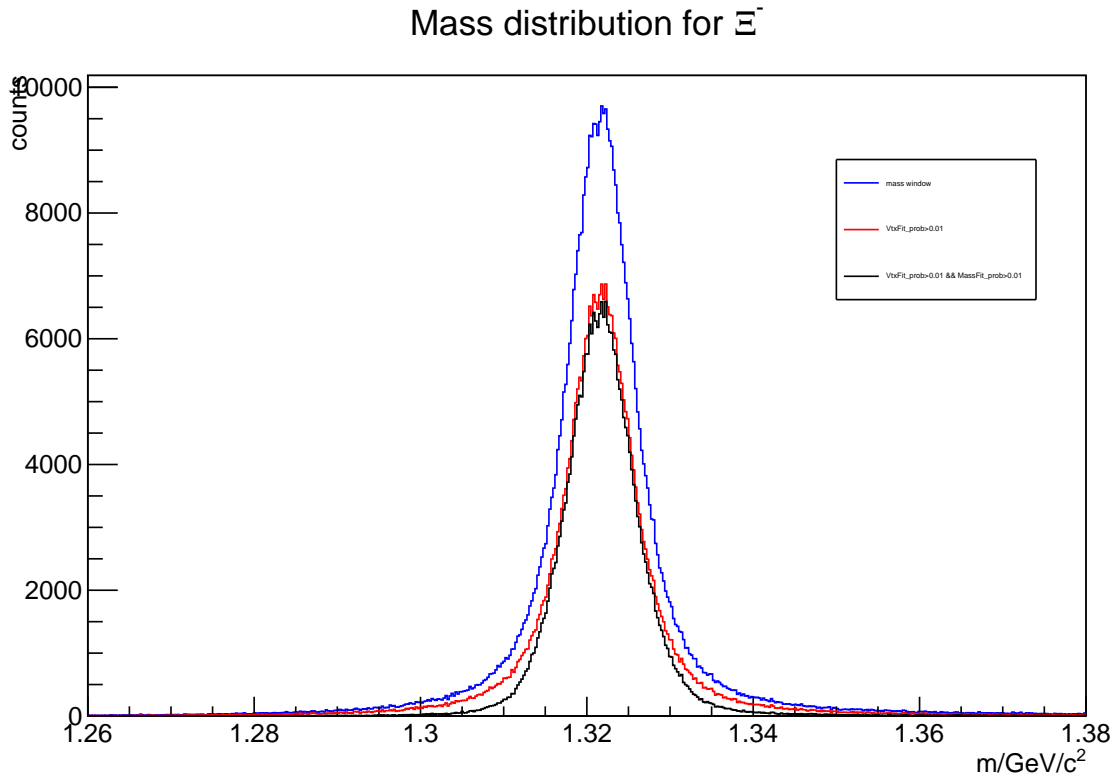


Figure 3.14: Mass distribution of Ξ^- for different cuts

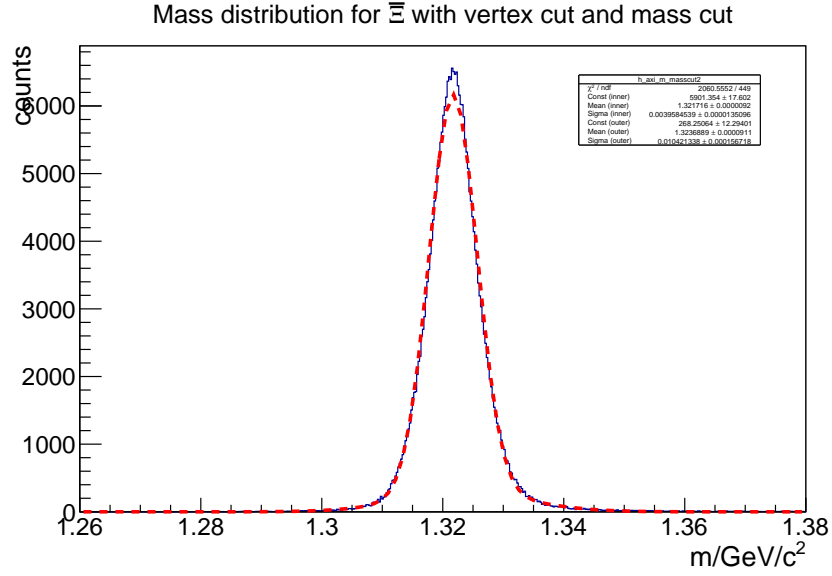


Figure 3.15: Mass fit with a double gaussian fit

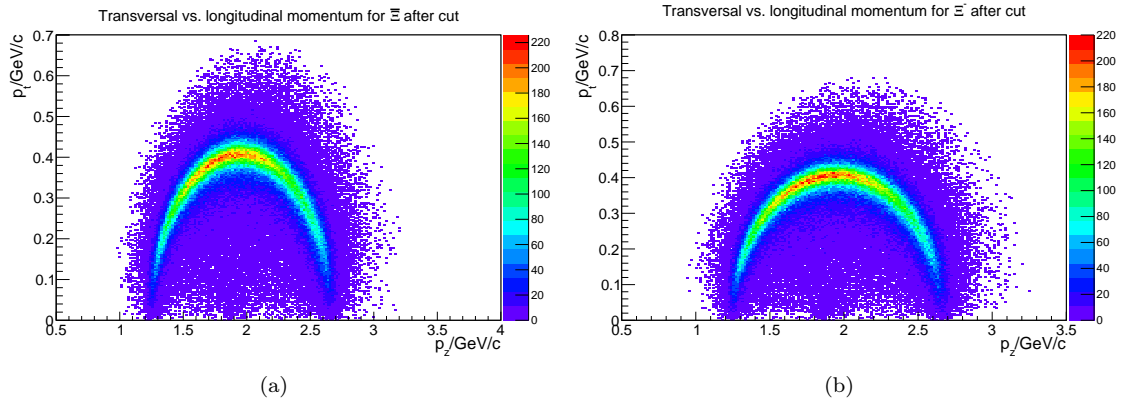


Figure 3.16: The plots shows the transverse against the longitudinal momentum for Ξ and Ξ^-

-the reconstruction efficiency for Ξ^- is 18.39% and for Ξ^0 18.64%

3.4 Reconstruction of $\Xi(1820)$ and $\Xi^0(1820)$

3.4.1 Combination

- daughter particles for $\Xi(1820)^-$: Λ^0 and K^- meson
- daughter particles for $\Xi^0(1820)$: $\bar{\Lambda}^0$ and K^+
- using best candidate from Λ^0 and $\bar{\Lambda}^0$
- K^+ and K^- with more than 3 Hits in one subdetector
- performing a mass window cut with width of $0.3\text{GeV}/c^2$

3.4.2 Fitting

- fitting particles to common vertex with PndKinVtxFitter
- fit information are given to PndKinFitter with mass constraint
- only select particles with prob bigger than 0.01 for both fitters
- scheme in figure 3.17
- if there is more than one particle, choose best candidate

3.5 Reconstruction of hole chain

3.5.1 combination

- using best candidate from $\Xi(1820)^-$ and Ξ^0
- for c.c : $\Xi^0(1820)$ and Ξ^-
- mass window of $0.3\text{GeV}/c^2$

3.5.2 Fitting

- use PndKinFitter with four momentum constrained
- initial four momentum vector is

$$(p_x, p_y, p_z, E) = (0, 0, 4.6, 5.63)$$

- if probability is better than 1% keep candidate
- scheme shown in figure 3.19
- table 3.4 shows summary of reconstruction efficiency for non-final state particles
- dalitz plot is shown in figure 3.20

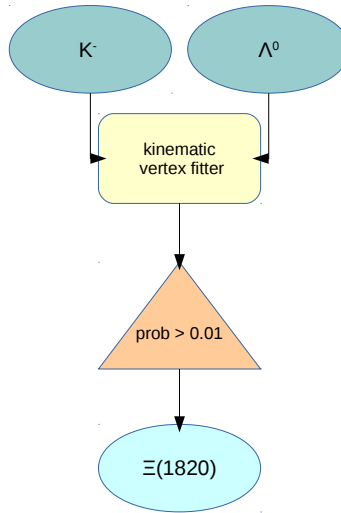


Figure 3.17: Scheme for $\Xi(1820)^-$ reconstruction

Figure 3.18: 4-constraint fit probability

Table 3.4: reconstruction efficiency for non-final state particles for $\bar{p}p \rightarrow \Xi(1820)^- \bar{\Xi}$

particle	reco efficiency in %	dp/p in %
Λ^0		
$\bar{\Lambda}^0$		
$\bar{\Xi}$		
$\Xi(1820)^-$		
$\bar{\Xi} \Xi$ system		

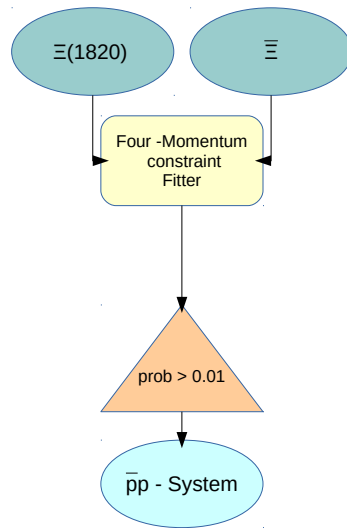


Figure 3.19: Scheme for 4-Constraint Fit

Figure 3.20: Dalitz plot for reconstructed particles

4 Background

Bibliography

[1] J. B. et al., *Particle Data Group*. Phys. Rev. D86, 010001, 2012.